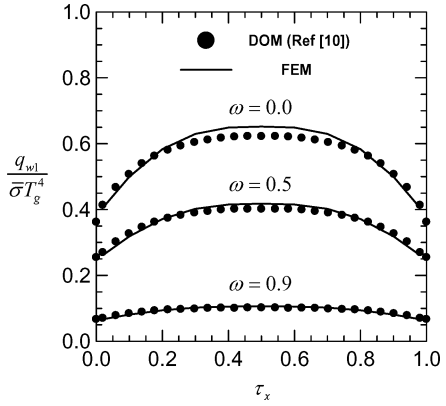

Fig. 3 Nondimensional net wall radiative heat flux in a black enclosure with an anisotropically scattering medium.

ray effect and false scattering. The discrepancies for the case of $\omega = 0.0$ are attributable to ray effect and false scattering. Even in the case of $\omega = 0.0$, the maximum relative error is less than 7%. In case 2, the number of iteration is less than six.

Conclusions

A finite element formulation based on the original discrete-ordinate equation is developed for the simulation of radiative heat transfer in absorbing and scattering media. Two cases of radiative heat transfer in two-dimensional rectangular enclosure filled with semitransparent media are examined to verify this new formulation. The results show that the finite element formulation presented in this Note has a good accuracy in solving the radiative heat transfer in absorbing and scattering media. In comparison with the conventional finite element method for radiative heat transfer, the new finite element formulation avoids the complex geometrical integration and can be used to solve the radiative heat transfer in anisotropically scattering media.

Acknowledgment

The support of this work by the National Nature Science Foundation of China (50336010) is gratefully acknowledged.

References

[1]Razzaque, M. M., Klein, D. E., and Howell, J. R., "Finite Element Solution of Radiative Heat Transfer in Two-Dimensional Rectangular Enclosure with Gray Participating Media," *Journal of Heat Transfer*, Vol. 105, No. 4, 1983, pp. 933–936.

[2]Lin, J. D., "Radiative Transfer Within an Arbitrary Isotropically Scattering Medium Enclosed by Diffuse Surfaces," *Journal of Thermophysics and Heat Transfer*, Vol. 2, No. 1, 1988, pp. 68–73.

[3]Anteby, I., Shai, I., and Arbel, A., "Numerical Calculations for Combined Conduction and Radiation Transient Heat Transfer in a Semitransparent Medium," *Numerical Heat Transfer, Part A*, Vol. 37, No. 4, 2000, pp. 359–371.

[4]Furmanski, P., and Bannaszek, J., "Finite Element Analysis of Concurrent Radiation and Conduction in Participating Media," *Journal of Quantitative Spectroscopy and Radiative Transfer*, Vol. 84, No. 3, 2004, pp. 563–573.

[5]Fiveland, W. A., and Jessee, J. P., "Finite Element Formulation of the Discrete-Ordinates Method for Multidimensional Geometries," *Journal of Thermophysics and Heat Transfer*, Vol. 8, No. 3, 1994, pp. 426–433.

[6]Modest, M. F., *Radiative Heat Transfer*, 2nd ed., Academic Press, San Diego, CA, 2003, pp. 498–530.

[7]Siegel, R., and Howell, J. R., *Thermal Radiation Heat Transfer*, 4th ed., Taylor and Francis, Philadelphia, 2002, pp. 681–695.

[8]Chai, J. C., Lee, H. S., and Patankar, S. V., "Improved Treatment of Scattering Using the Discrete Ordinates Method," *Journal of Heat Transfer*, Vol. 116, No. 1, 1994, pp. 260–263.

[9]Ratzel, A. C., and Howell, J. R., "Two-Dimensional Radiation in Absorbing-Emitting Media Using the P-N Approximation," *Journal of Heat Transfer*, Vol. 105, No. 2, 1983, pp. 333–340.

[10]Kim, T. K., and Lee, H., "Effect of Anisotropic Scattering on Radiative Heat Transfer in Two-Dimensional Rectangular Enclosures," *International Journal of Heat and Mass Transfer*, Vol. 31, No. 8, 1988, pp. 1711–1721.

Laminar Flow Through a Staggered Tube Bank

You Qin Wang*
University of Northern British Columbia, Prince George, British Columbia V2N 4Z9, Canada

Nomenclature

C_f	=	friction coefficient
C_p	=	specific heat, J/kg/K
D	=	tube diameter, m
f_c	=	average friction factor
L_{ds}	=	downstream length, m
L_{tb}	=	tube bank length, m
L_{us}	=	upstream length, m
N_L	=	number of tube rows
Nu_{LM}	=	average Nusselt number
P	=	pressure, N/m^2
Pr	=	Prandtl number ($=\mu C_p/k$)
$Re_{\max}$	=	Reynolds number based on the maximum velocity ($=\rho V_{\max} D/\mu$)
S_L	=	longitudinal pitch, m
S_T	=	transverse pitch, m
T	=	temperature, K
u_*	=	friction velocity, m/s
$V_{\max}$	=	average velocity at minimum flow cross section
y	=	wall coordinate, m
y^+	=	wall unit or nondimensional wall coordinate ($=yu_*/\nu$)
Δy	=	distance measured from the first node to the wall, m
Δy^+	=	the first node's wall unit ($=\Delta y u_*/\nu$)
μ	=	fluid dynamic viscosity, (kg/m) s^{-1}
ρ	=	fluid density, kg/m^3

Subscripts

out	=	outlet condition
w	=	tube wall
∞	=	inlet condition

Introduction

STUDY of flow and heat transfer in tube bundles has a variety of applications in industry. Considerable effort has been spent on both experimental investigation and numerical simulation, as summarized in an earlier paper.[1] The purpose of this study is to establish that an in-house computational fluid dynamics (CFD) program is accurate by comparing results obtained with the software FLUENT with solutions obtained in the numerical study recently conducted by Wang et al.[1] The solutions for $Re_{\max} = 100$ and 300 at a nominal pitch-to-diameter ratio of 1.5 are compared.

Problem Description

The flow is modeled as two-dimensional axisymmetric. The tube arrangements and the solution domain are illustrated in Figs. 1a and 2a of Ref. 1. The longitudinal pitch S_L of the tube bank is equal

Received 11 August 2003; revision received 20 January 2004; accepted for publication 31 January 2004.

*High Performance Computing Research Associate, Computing and Telecommunications Services, 3333 University Way; yqwang@unbc.ca.

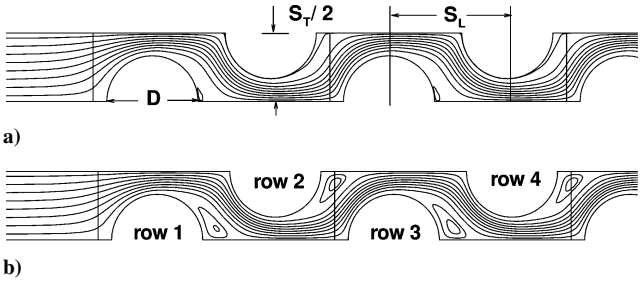

Fig. 1 Streamlines near the inlet region: a) $Re_{\max} = 100$ and b) $Re_{\max} = 300$.

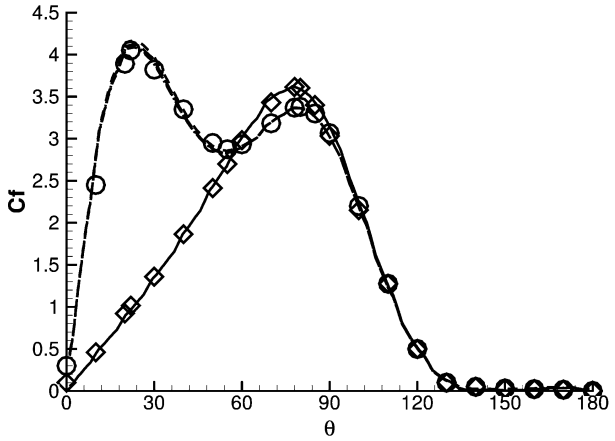

Fig. 2 Skin friction coefficient distributions on the first four tubes: ——, FLUENT, row 1; –·–·–, FLUENT, row 2; – – –, FLUENT, row 3; –··–··–, FLUENT, row 4; - - - -, FLUENT, periodic bc; ◇, Ref. 1, row 1; and ○, Ref. 1, rows 2–4.

to 1.2990 m, whereas the transverse pitch S_T of the tube bank is equal to 1.50 m. Tube diameter D is equal to 1 m. $L_{\text{us}} = 4.875$ m, $L_{\text{tb}} = 11.691$ m, and $L_{\text{ds}} = 23$ m.

The Prandtl number Pr is equal to 0.74. The Reynolds number $Re_{\max}$, based on the maximum velocity, is defined by $Re_{\max} = \rho V_{\max} D/\mu$. A uniform velocity and a constant temperature are used for inlet boundary conditions. The pressure-outlet condition in FLUENT is employed. The use of a pressure-outlet boundary condition instead of an outflow condition often results in a better rate of convergence if backflow occurs during iteration. Default settings for pressure-outlet boundary conditions are used (gauge pressure $= 0\text{N/m}^2$; backflow total temperature $= 300$ K). It should be noted that the static-pressure value used here is relative to the operating pressure set in the Operating Conditions panel. The outflow boundary condition, another boundary condition option in FLUENT, is tested in the present study. It has been found that although there is no recirculation through the outflow boundary at any point during the calculations in the present study, the use of a pressure-outlet boundary condition instead of an outflow condition still results in a better rate of convergence. A combination of symmetry and no-slip tube surfaces is used on the bottom and top boundaries. The temperature of the tube wall (T_w) is 400 K and the bulk temperature of the crossflow air (T_∞) is 300 K.

Quadrilateral cells were used around the tube wall and triangular cells were used in all other regions. The total number of cells is 48,304. To evaluate the friction velocity u_* accurately, Δy is set to 0.01 m around all tubes so that the maximum value of Δy^+ is less than 0.5. Solution-adaptive refinement, a feature of FLUENT, was used to establish the grid independence of the present results, although the results of the grid-independence tests are not shown in this Note. Convergence was declared when the maximum scaled residuals were less than 1×10^{-5} for the continuity equation, x-velocity equation, and y-velocity equation and less than 1×10^{-6} for the energy equation. For $Re_{\max} = 100$, after 675 iterations, the calculation met the convergence criteria. After 200 more iterations, the four residuals decreased by 15% but the solution differed between the two results by a maximum of 0.08% for the skin-friction coefficient around the first tube.

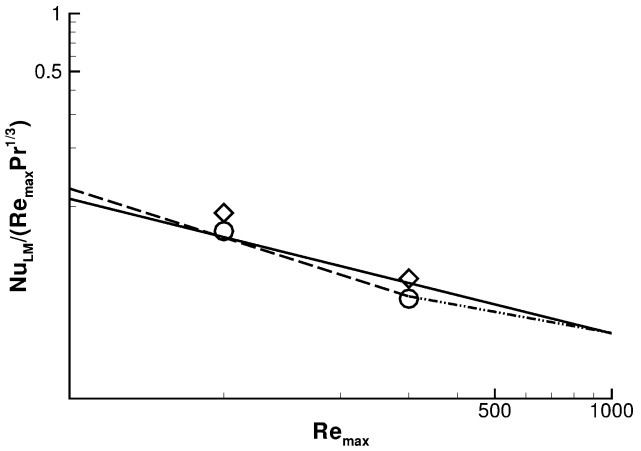

Fig. 3 Average heat transfer results compared with empirical correlations: ○, FLUENT; ◇, Ref. 1; ——, Eq. (1); – – –, Eq. (2); and –··–··–, Eq. (3).

Results

Streamlines near the inlet region for $Re_{\max} = 100$ and 300 are shown in Figs. 1a and 1b, respectively. The plots match well with Figs. 4b and 5a in Ref. 1. The streamlines after the last tube and isotherms near the inlet region, not shown here, also match well with plots in Figs. 4a, 4c, and 5b of Ref. 1.

The C_f distributions for $Re_{\max} = 100$ are shown in Fig. 2. The agreement between the present results (FLUENT) and those of Wang et al.[1] (in-house CFD code) is remarkably good, the maximum deviation being approximately 1.5%. The result obtained using the periodic boundary condition (a feature of FLUENT) has also been plotted in Fig. 2 and it matches well with the results for the tubes in rows 2–4. In particular, the first and second peaks are accurately located in the same place for all simulations.

The dimensionless pressure distributions along the bottom and top domain boundaries for the region around the first four tube rows match well with Fig. 10a of Wang et al.,[1] although the plot has not been shown in this note.

In the present study, the average Nusselt number Nu_{LM} is averaged among the surfaces of the first 10 tubes. Simulation results with the empirical correlations of Žukauskas et al.[2] and the Engineering Sciences Data Unit (ESDU)[3] are plotted in Fig. 3. The empirical correlation of Žukauskas et al.[2] and the empirical correlation of ESDU[3] have the same value (0.069) for $Re_{\max} = 100$, and the relative errors based on this value are 7.2 and 33.3%, respectively, for the present study and the previous study of Wang et al.[1] For $Re_{\max} = 300$, the empirical correlation coefficient of Žukauskas et al.[2] and the empirical correlation coefficient of ESDU[3] are 0.040 and 0.034, respectively. The relative errors based on 0.040 are 17.5 and 5.0%, respectively, for the present study and the study of Wang et al.[1] The relative errors based on 0.034 are 2.9 and 23.5%, respectively, for the present study and the study of Wang et al.[1]

The Žukauskas et al.[2] correlations used in Fig. 3 are the 16-row staggered bundle equations from Table 2 of Ref. 2 with the correction (equal to 0.979) for 10 rows

$$\frac{Nu_{\text{LM}}}{Re_{\max} Pr^{\frac{1}{3}}} = 0.979\left(0.71 Re_{\max}^{-0.5} Pr^{0.0267}\right) \tag{1}$$

As indicated in Ref. 4, the range of Eq. (1) is $40 < Re_{\max} \leq 1000$.

The ESDU correlations used in Fig. 3 are for a 10-row staggered bundle from Table 1 of Ref. 3:

$$\frac{Nu_{\mathrm{LM}}}{Re_{\max} Pr^{\frac{1}{3}}} = 1.309\left(1.04 Re_{\max}^{-0.64} Pr^{0.00667}\right) \tag{2}$$

$$\frac{Nu_{\mathrm{LM}}}{Re_{\max} Pr^{\frac{1}{3}}} = 0.273\left(0.71 Re_{\max}^{-0.365} Pr^{0.00667}\right) \tag{3}$$

The ranges of Eqs. (2) and (3) are $10 \le Re_{\max} \le 300$ and $300 < Re_{\max} \le 20{,}000$, respectively.

Finally, a comparison of the present study prediction of average friction factor, f_c, with an empirical correlation is made. Here f_c is defined by $f_c = (P_\infty - P_{\mathrm{out}})/(2\rho V_{\max}^2 N_L)$, where the number of tube rows N_L was 10. The empirical correlation is Eq. (46) of Ref. 5:

$$f_c = 0.25\left[0.0683 + \frac{111}{Re_{\max}} - \frac{97.3}{(Re_{\max})^2} + \frac{426}{(Re_{\max})^3} - \frac{574}{(Re_{\max})^4}\right] \tag{4}$$

The range of Eq. (4) is $3 \le Re_{\max} \le 1000$. The values obtained from Eq. (4) for $Re_{\max} = 100$ and 300 are 0.445923 and 0.262984, respectively; and in the present study, the f_c values are 0.445925 and 0.262984 for $Re_{\max} = 100$ and 300, respectively. The relative error based on the values obtained from Eq. (4) is smaller than 0.0005% for both Reynolds numbers.

Conclusions

The accuracy of the in-house CFD program for predicting a two-dimensional laminar flow through a staggered tube bank has been established by comparing the current results obtained with FLUENT to the solutions obtained in the numerical study recently conducted by Wang et al.[1] In particular, the solutions for $Re_{\max} = 100$ and 300 at a nominal pitch-to-diameter ratio of 1.5 are compared. The solutions obtained with FLUENT, including the contour plots of isotherms, streamlines, and skin-friction-coefficient distributions, compared well with previous numerical solutions[1] obtained by the in-house CFD program, as did the dimensionless-pressure profiles along the bottom and top boundaries. Furthermore, the average heat-transfer coefficients and average friction factors obtained with both FLUENT and the in-house program match well with established empirical correlations. It can, therefore, be concluded that the in-house CFD program can be used to obtain flow and temperature fields for geometries and conditions similar to those of the present problem.

Acknowledgments

This work was supported by Canada Foundation for Innovation (Project 1854; Institute: University of Northern British Columbia). Simulations were performed on an SGI Origin 3400 at the University of Northern British Columbia.

References

[1]Wang, Y. Q., Penner, L. A., and Ormiston, S. J., "Analysis of Laminar Forced Convection of Air for Crossflow in Banks of Staggered Tubes," *Numerical Heat Transfer, Part A*, Vol. 38, No. 8, 2000, pp. 819–845.

[2]Žukauskas, A., Skrinska, A., Žiugzda, J., and Gnielinski, V., "Single-Phase Convective Heat Transfer: Banks of Plain and Finned Tubes," *Heat Exchanger Design Handbook*, edited by G. Hewitt, Begell House, New York, 1998, Chap. 2.5.3.

[3]Engineering Sciences Data Unit, "Convective Heat Transfer During Crossflow of Fluids over Plain Tube Banks," Series of Heat Transfer, Vol. 2, Rept. 73031, IHS Group, ESDU International, London, Nov. 1973.

[4]Žukauskas, A., and Ulinskas, R., "Efficiency Parameters for Heat Transfer in Tube Banks," *Heat Transfer Engineering*, Vol. 6, No. 1, 1985, pp. 19–25.

[5]Žukauskas, A., and Ulinskas, R., "Single-Phase Fluid Flow: Banks of Plain and Finned Tubes," *Heat Exchanger Design Handbook*, edited by G. Hewitt, Begell House, New York, 1998, Chap. 2.2.4.

Thermoeconomical Optimization of Double-Pipe Heat Exchanger for Waste Heat Recovery

M. S. Söylemez*
University of Gaziantep, 27310 Gaziantep, Turkey

Nomenclature

A	=	area of the double-pipe heat exchanger (DPHE), m^2
A_{opt}	=	optimum area of the DPHE, m^2
a_0	=	fixed parameter used in Eq. (14) $[=\rho_i C_{p,i} V_i/(\rho_o C_{\mathrm{po}} V_o)]$
a_1	=	fixed parameter used in Eq. (12) $[=P_1 C_E H(Q/L)^2/(P_2 C_A \Delta T_{\max} \pi^2)]$
a_2	=	fixed parameter used in Eq. (13) $\{=0.023 Pr_i^{0.3} k_i [4/(\propto_i \pi)]^{0.8}\}$
a_3	=	fixed parameter used in Eq. (15) $(=0.023 Pr_o^{0.4} k_o \{4b/(\propto_o \pi)/[1+(1+a_0)^{0.5}]\}^{0.8}/[(1+a_0)^{0.5}-1])$
a_4	=	fixed parameter used in Eq. (16) $[=a_2 a_3 b^{0.8}/(a_2 + a_3 b^{0.8})]$
a_5	=	fixed parameter used in Eq. (17) $[=(a_1/a_4)^{1.25}]$
a_6	=	fixed parameter used in Eq. (18) $\{=0.31/[4a_5/(\propto_i \pi)]^{0.25}\}$
a_7	=	fixed parameter used in Eq. (19) $(=0.31/\{4ba_5/(\propto_o \pi)/[1+(1+a_0)^{0.5}]\}^{0.25})$
a_8	=	fixed parameter used in Eq. (22) $\{=a_6 + bca_7/[(1+a_0)^{0.5}-1]\}$
a_9	=	fixed parameter used in Eq. (22) $[=8a_8 a_5^3 P_1 C_{\mathrm{EL}} H(L_{\mathrm{eq}}/L)/(\eta_p \eta_m \pi^2 \rho_i^2)]$
a_{10}	=	fixed parameter used in Eq. (23) $(=P_2 C_A \pi)$
a_{11}	=	fixed parameter used in Eq. (28) $[=4a_5/(\propto_i \pi)]$
a_{12}	=	fixed parameter used in Eq. (28) $\{=4ba_5/[1+(1+a_0)^{0.5}]/(\propto_o \pi)\}$
a_{13}	=	fixed parameter used in Eq. (36) $[=4m_i/(\propto_i \pi)]$
a_{14}	=	fixed parameter used in Eq. (36) $\{=4bm_i/[1+(1+a_0)^{0.5}]/(\propto_o \pi)\}$
a_{15}	=	fixed parameter used in Eq. (38) $[=512 P_1 C_{\mathrm{EL}} H m_i^3 (L_{\mathrm{eq}}/L)(1/a_{13} + bc/a_{14})/(\eta_p \eta_m \pi^2 \rho_i^2)]$
b	=	fixed parameter used in Eq. (15) $(=C_{p,i}/C_{p,o})$
C	=	thermal capacity ratio $[=m_i C_{p,i}/(m_o C_{p,o})]$
C_A	=	area dependent first cost of the DPHE, \$/m^2
C_E	=	cost of energy recovered by the DPHE, \$/W · hr
C_{EL}	=	cost of electricity, \$/(W · hr)
C_i	=	heat capacity rate of flowing fluid in inner pipe of DPHE, W/K
$C_{\max}$	=	higher heat capacity rate of flowing fluid in DPHE, W/K
$C_{\min}$	=	lower heat capacity rate of flowing fluid in DPHE, W/K
C_o	=	heat capacity rate of flowing fluid in the annulus part of DPHE, W/K
$C_{p,i}$	=	specific heat of flowing fluid in inner pipe of DPHE, J/(kg · K)

Received 31 October 2003; revision received 30 June 2004; accepted for publication 1 July 2004.

*Associate Professor, Department of Mechanical Engineering; sait@gantep.edu.tr.